International Journal of Biological Macromolecules 282 (2024) 136873

Contents lists available at ScienceDirect

International Journal of Biological Macromolecules

journal homepage: www.elsevier.com/locate/ijbiomac

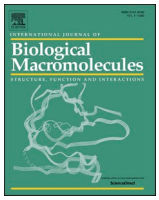

# Exploring the binding mode of phenyl and vinyl boronic acids to human carbonic anhydrases

Davide Esposito [a], Simona Maria Monti [a], Claudiu T. Supuran [b], Jean-Yves Winum [c], Giuseppina De Simone [a,*], Vincenzo Alterio [a,*]

[a] Institute of Biostructures and Bioimaging, Consiglio Nazionale delle Ricerche (IBB-CNR), Via Pietro Castellino, 111, 80131 Naples, Italy
[b] Department of NEUROFARBA - Section of Pharmaceutical and Nutraceutical Sciences, University of Florence, Sesto Fiorentino, Florence, Italy
[c] IBMM, University of Montpellier, CNRS, ENSCM, Montpellier, France

ARTICLE INFO

*Keywords:*
Boronic acid
Carbonic anhydrase inhibitors
X-ray crystallography

ABSTRACT

Boronic acids are an interesting but still poorly studied class of carbonic anhydrase inhibitors. Previous investigations proved that derivatives incorporating aromatic, arylalkyl, and arylalkenyl moieties are low micromolar to millimolar inhibitors for several α- and β-CAs involved in pathologic states.

Here we report a high-resolution X-ray study on two classes of boronic acids (phenyl and vinyl) in complex with hCA II. Our results unambiguously clarify the binding mode of these molecules to the human carbonic anhydrase active site, which occurs through their tetrahedral anionic form, regardless of the nature of the organic scaffold. Data here presented contribute to the understanding of the inhibition mechanism of boronic acids that can be fruitfully used for the rational design of novel and effective isozyme-specific carbonic anhydrase inhibitors.

## 1. Introduction

Boronic acids are organic compounds that contain a trivalent boron atom bonded to a carbon atom and two hydroxyl groups, arranged in a trigonal planar geometry [1]. These molecules have peculiar chemical properties. Indeed, since the boron atom has only six valence electrons, boronic acids act as mild organic Lewis acids forming in water tetrahedral adducts with a carbon-like configuration. In these adducts a negative charge is formally assigned to the boron atom, but in fact delocalized on the three heteroatoms [1] (Scheme 1).

Boronic acids can be classified as alkyl-, alkenyl-, alkynyl-, and aryl-derivatives depending on the nature of the R-group directly bonded to the boron atom, which significantly influences the chemical properties of the molecules, including their acidity [1,2]. These compounds are highly attractive for synthetic purposes since they exhibit a moderate reactivity profile, are stable and are easy to handle. Moreover, they are considered "green" compounds due to their low toxicity and their degradation into the environmentally friendly boric acid [1]. They are also very promising tools in medicinal chemistry and various boron-based compounds have shown remarkable efficacy as anticancer, antibacterial, antiviral, and antiparasitic agents, among others [3–7]. Indeed, some boronic acid-based drugs have been approved by Food and Drug Administration and by European Medicines Agency for the treatment of several pathologies, such as Bortezomib and Ixazomib for multiple myeloma therapy [3,8–10]. Additionally, others are under investigation in clinical trials, such as Dutogliptin for the treatment of diabetes mellitus (type II), Delanzomib which has been in phase II clinical trials for the treatment of multiple myeloma, and Talabostat which is currently in phase II trial for treatment of advanced solid cancers (NCT04171219) [10–12] (Fig. 1).

Carbonic anhydrases (CAs) are ubiquitous metalloenzymes, present in most living organisms, which catalyze the reversible hydration of carbon dioxide to bicarbonate and proton [13–15]. Fifteen different isoforms have been identified in humans, which differ in catalytic properties, cellular localization and tissue distribution, and have been shown to be involved in a large number of physio/pathological processes [16,17]. For this reason, many human CAs (hCAs) have been recognized as important targets for the design of inhibitors with biomedical applications [13]. To date, the most investigated CA inhibitors (CAIs) are aromatic/heterocyclic sulfonamides, some of which have found applications as diuretics, anti-epileptics, antiglaucoma, anti-obesity, and anticonvulsant agents [17]. Others are currently being

* Corresponding authors.
*E-mail addresses:* giuseppina.desimone@cnr.it (G. De Simone), vincenzo.alterio@cnr.it (V. Alterio).

https://doi.org/10.1016/j.ijbiomac.2024.136873
Received 3 September 2024; Received in revised form 20 October 2024; Accepted 22 October 2024
Available online 23 October 2024

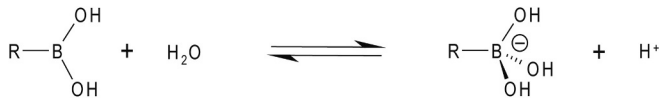

**Scheme 1.** Ionization equilibrium of boronic acids in water

investigated in clinical trials, such as SLC-0111, which is in Phase Ib/II clinical trials for the treatment of advanced metastatic solid tumors [18,19]. However, these drugs often lack selectivity against the different isoforms; therefore, the development of more selective CAIs is an ever-growing research field. To this end, a huge number of new classes of inhibitors, alternative to sulfonamides, have been investigated, resulting in the production of new CAIs, some of which exhibit very promising properties. For example, coumarins were demonstrated to be highly selective inhibitors of the tumor associated isoforms hCA IX and hCA XII and showed significant capabilities in inhibiting tumor metastasis in experimental models [20].

Boronic acids have been scarcely explored as CAIs. The first CA inhibition studies on such compounds were carried out using phenyl boronic acid ($PhB(OH)_2$), which showed millimolar inhibition properties against most hCA isoforms [21–23]. Subsequently, inhibition assays were conducted on a series of derivatives incorporating aromatic, arylalkyl, and arylalkenyl moieties against human α-CAs (isoforms I, II, IX, and XII) and β-CAs from the pathogenic fungi *Cryptococcus neoformans* (Can2) and *Candida albicans* (Nce103) [24,25]. These assays confirmed the CA inhibition capability of such compounds and highlighted the essential role of the R-group in determining the inhibition potency of these molecules, which ranged from low micromolar to millimolar inhibitors [24,25]. More recently, the peptidomimetic proteasome inhibitor Bortezomib was also assayed as an inhibitor of hCAs and many β-CAs from pathogenic fungi, bacteria, insects, and plants, revealing inhibition constants in the micromolar range [26–28]. Surprisingly, although these data strongly indicated the potential of boronic acids in the development of new CAIs, the inhibition mechanism of these molecules remained unstudied for a long time. Only in 2024 Rasheed and coworkers reported the crystallographic structure at 2.60 Å resolution of the phenyl-boronic acid derivative 1 (Fig. 2) in complex with hCA II [29], providing a first structural hypothesis on the binding mode of these molecules to the CA active site.

In particular, these authors concluded that compound 1 bound to the hCA II active site with the boron atom in its trigonal planar form (Fig. 3) [29]. This finding was quite surprising to us, as several previous studies indicated the capability of boronic acids to form complexes with Lewis bases, such as hydroxide anions, and electron-donating groups, like OH moieties of Ser or Thr residues from enzyme active sites, leading to tetrahedral species [3,10,30–34]. Thus, due to the presence of the highly nucleophilic zinc-bound hydroxide ion in hCA II, the formation of a tetrahedral B(III) species coordinated to the catalytic zinc ion, was expected [24]. This discrepancy prompted us to further investigate this peculiar class of CAIs carrying out detailed structural studies. Here, by determining the high-resolution crystal structures of two different types of boronic acids (phenyl and vinyl) in complex with hCA II, we elucidate the binding mode of this class of CAIs to the active site of hCAs, paving the way for further investigations of these molecules in the development of isoform-selective CAIs.

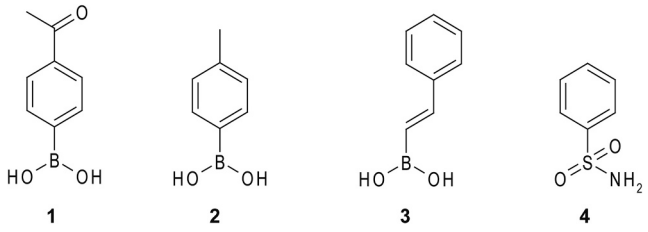

**Fig. 2.** Chemical structures of selected CAIs.

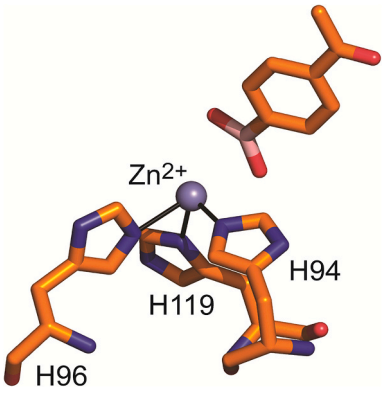


**Fig. 3.** Active site view of hCA II/1 adduct (PDB code 8IGF) [29].

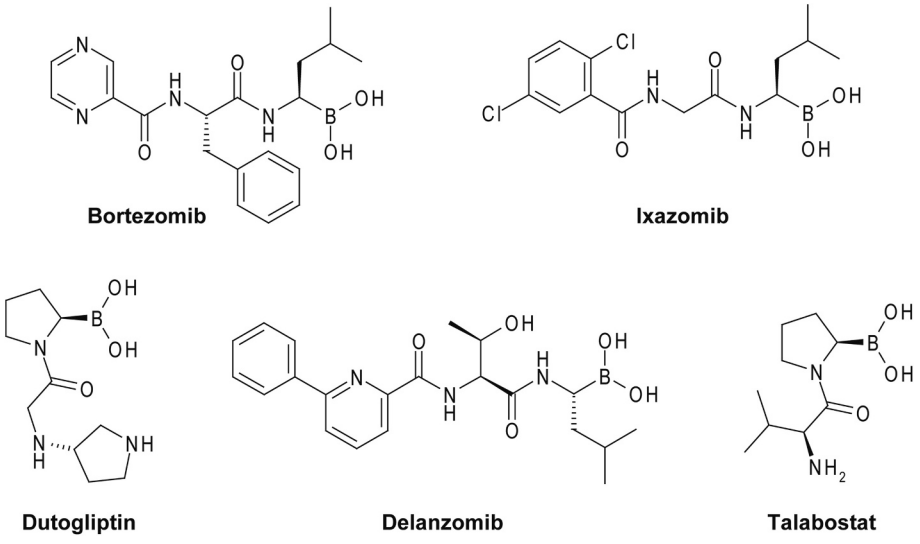


**Fig. 1.** Chemical structures of some boronic acid-based approved drugs or in clinical trials.

**Table 1**
Data collection and refinement statistics for the hCA II/inhibitor adducts.

| *Crystal parameters* | hCA II/2 (pH = 8.5) (PDB code 9GFV) | hCA II/2 (pH = 7.4) (PDB code 9GFW) | hCA II/3 (PDB code 9GFX) |
|---|---|---|---|
| Space group | $P2_1$ | $P2_1$ | $P2_1$ |
| a (Å) | 42.54 | 42.20 | 42.48 |
| b (Å) | 41.36 | 41.44 | 41.52 |
| c (Å) | 72.25 | 72.08 | 72.56 |
| β (°) | 104.3 | 104.4 | 104.4 |
| *Data collection statistics* | | | |
| Resolution (Å) | 35.6–1.14 (1.16–1.14) | 40.9–1.07 (1.09–1.07) | 41.2–1.35 (1.37–1.35) |
| Temperature (K) | 100 | 100 | 100 |
| Total reflections | 259,767 | 600,889 | 339,153 |
| Unique reflections | 87,111 (4,208) | 103,340 (4,889) | 54,273 (2,703) |
| Completeness (%) | 98.1 (96.1) | 97.1 (92.3) | 100 (100) |
| <I>/<σ(I)> | 13.8 (2.1) | 17.8 (4.5) | 14.8 (3.1) |
| Redundancy (%) | 3.0 (2.6) | 5.8 (4.6) | 6.2 (6.0) |
| $R_{merge}$ [a] | 0.078 (0.475) | 0.074 (0.371) | 0.104 (0.605) |
| $R_{meas}$ [a] | 0.095 (0.596) | 0.081 (0.422) | 0.114 (0.661) |
| $R_{pim}$ [a] | 0.052 (0.355) | 0.032 (0.199) | 0.044 (0.262) |
| CC1/2 [b] | 0.989 (0.703) | 0.998 (0.916) | 0.996 (0.803) |
| *Refinement statistics* | | | |
| Resolution (Å) | 35.6–1.14 | 40.9–1.07 | 41.2–1.35 |
| $R_{work}$ [c] (%) | 12.9 | 14.1 | 12.6 |
| $R_{free}$ [c] (%) | 14.5 | 16.2 | 14.8 |
| r.m.s.d. from ideal geometry: | | | |
| Bond lengths (Å) | 0.014 | 0.013 | 0.014 |
| Bond angles (°) | 1.9 | 1.9 | 2.1 |
| Number of protein atoms | 2,048 | 1,058 | 2,048 |
| Number of inhibitor atoms | 11 | 11 | 12 |
| Number of water molecules | 219 | 209 | 190 |
| Average B factor (Å$^2$) | | | |
| All atoms | 10.9 | 11.7 | 14.3 |
| Protein atoms | 9.8 | 10.9 | 13.4 |
| Inhibitor atoms | 10.1 | 12.4 | 18.4 |
| Water molecules | 21.5 | 20.0 | 24.0 |

[a] $R_{merge} = \Sigma_{hkl}\Sigma_i|I_i(hkl) - < I(hkl) >|/\Sigma_{hkl}\Sigma_i I_i(hkl)$; $R_{meas} = \Sigma_{hkl}\{n(hkl)/[n(hkl)-1]\}^{1/2}\Sigma_i|I_i(hkl) - < I(hkl) >|/\Sigma_{hkl}\Sigma_i I_i(hkl)$; $R_{pim} = \Sigma_{hkl}\{1/[n(hkl)-1]\}^{1/2}\Sigma_i|I_i(hkl) - < I(hkl) >|/\Sigma_{hkl}\Sigma_i I_i(hkl)$, where $I_i(hkl)$ is the intensity of an observation and $< I(hkl) >$ is the mean value for its unique reflection; summations are over all "n" reflections.

[b] $CC1/2 = [\Sigma_i(a_i - < a >)/\Sigma_i(b_i - < b >)]/[\Sigma_i(a_i - < a >)^2\ \Sigma_i(b_i - < b >)^2]^{1/2}$; where $a_i$ and $b_i$ are the intensities of unique reflections merged across the observations randomly assigned to subsets A and B, respectively, and $< a >$ and $< b >$ are their averages.

[c] $R_{work} = \Sigma_h||F_o(h)| - |F_c(h)||/\Sigma_h|F_o(h)|$, where $F_o$ and $F_c$ are the observed and calculated structure-factor amplitudes, respectively. $R_{free}$ was calculated with 2.0 % (hCA II/2, pH = 8.5), 2.1 % (hCA II/2, pH = 7.4) or 2.9 % (hCA II/3) of the data excluded from the refinement.

## 2. Material and methods

### 2.1. Crystallization and data collection

hCA II native crystals were grown at 20 °C using the hanging drop vapor diffusion method. Two precipitant solutions were used to obtain suitable crystals at different pH values. In particular, for crystals obtained at pH 8.5, we used a crystallization condition containing 1.3 M sodium citrate and 0.1 M Tris-HCl, whereas for crystals obtained at pH 7.4, we used a reservoir solution consisting of 2.8 M $(NH_4)_2SO_4$, 50 mM Tris-HCl, and 5 mM 4-(hydroxymercurybenzoate). In both cases equal volumes of protein (10 mg/mL) and precipitant solution were mixed and equilibrated against 0.5 mL reservoir containing the same precipitant solution. Crystals grew within two days up to an average size of 0.3 mm × 0.3 mm × 0.2 mm. All complexes were obtained by the soaking technique. In particular, 1 M DMSO stock solution of each inhibitor was diluted up to 40 mM in the precipitant solution, containing up to 10–15 % (*v*/v) glycerol as cryoprotectant. Few hCA II native crystals were transferred and kept overnight in a 2 μL drop of these freshly prepared inhibitor solutions. Complete sets of diffraction data were collected at 100 K, at the Synchrotron source Elettra in Trieste, Italy, using the Dectris Pilatus 6 M detector. Intensity data were processed and scaled using the program HKL3000 [35]. Data collection statistics are shown in Table 1.

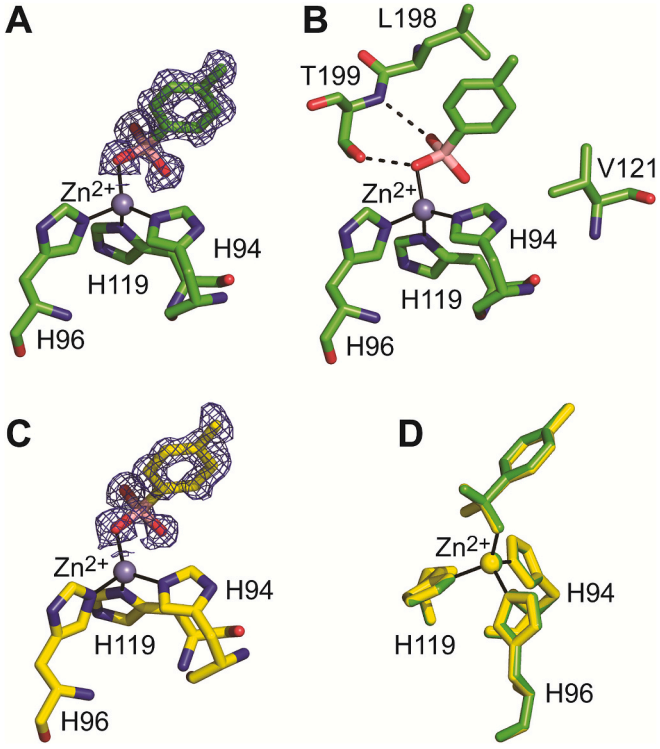


**Fig. 4.** Active site region of the hCA II/2 complex crystallized at pH 8.5 (A, B) or pH 7.4 (C). D) Structural superposition of the hCA II/2 adducts crystallized at pH 8.5 (green) and pH 7.4 (yellow). In A and C the σA-weighted (2Fo-Fc) map contoured at 1.0 σ, relative to the inhibitor molecule is shown. In B residues involved in hydrogen bonds and hydrophobic interactions (<4 Å) are displayed. In all panels continuous lines indicate zinc ion coordination, whereas dashed lines indicate hydrogen bond distances.

### 2.2. Structure determination and refinement

Initial phases of the three hCA II/inhibitor complexes were calculated using the PDB entry 1CA2 [36] with waters removed. The structures were refined using the program REFMAC5 [37], whereas model building and map inspections were performed using the program O [38]. Several rounds of restrained refinement and anisotropic temperature factor refinement alternated with manual rebuilding were necessary to reduce the crystallographic R-work/R-free values to the ones reported in Table 1. The stereochemical quality of the three models was finally assessed using Procheck [39] and Whatcheck [40] programs. Coordinates and structure factors have been deposited in the Protein Data Bank (accession codes are reported in Table 1).

## 3. Results and discussion

To clarify the binding mode of boronic acids to hCAs, we selected a

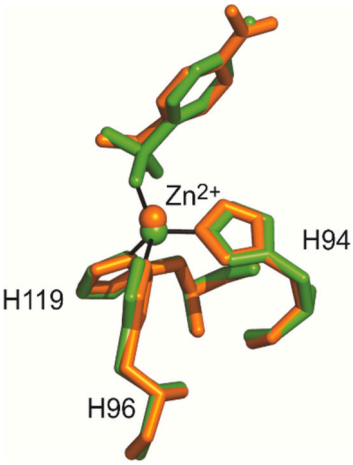


**Fig. 5.** Structural superposition of the active sites of hCA II/1 (orange) and hCA II/2 (green) adducts.

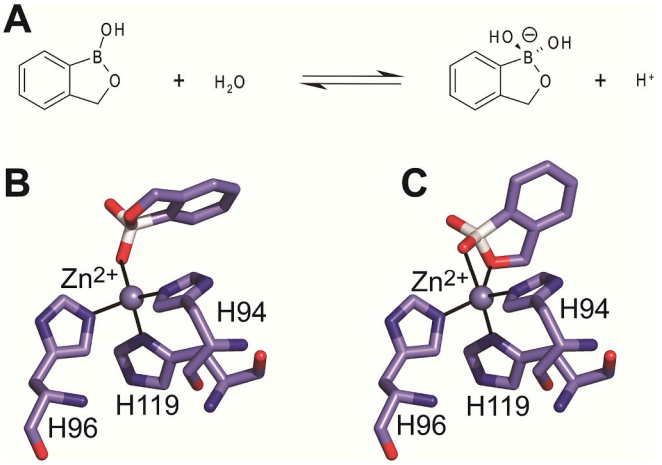


**Fig. 6.** A) Ionization equilibrium of benzoxaborole in water; B,C) details of the binding modes of benzoxaborole to the zinc ion in the hCA II active site. Two binding modes were observed: monodentate (B) and bidentate (C) (PDB code 5JQ0) [51].

micromolar hCA II inhibitor ($K_I$ 10.8 μM) from a series of compounds previously investigated by Winum and collaborators [24]. This compound, 4-methylphenyl-boronic acid (compound 2 in Fig. 2), which has a chemical structure very similar to 1, was characterized in its complex with hCA II using X-ray crystallography. Crystals of the hCA II/2 adduct were obtained following a procedure well described in the literature [41–45]. In particular, native hCA II was crystallized by the hanging drop vapor diffusion method at pH 8.5, and the obtained crystals were soaked in the precipitant solution containing the inhibitor at a concentration of 40 mM. Data were collected up to 1.14 Å resolution. Interestingly, the analysis of the electron density maps in the enzyme active site, from the early stages of crystallographic refinement, revealed features compatible with the binding of the inhibitor in its tetrahedral anionic form (Scheme 1 and Fig. 4A), differing from what reported in the study of Rasheed and colleagues [29]. In detail, the boronate moiety was tetrahedrally coordinated to the catalytic zinc ion through one oxygen atom, which was also involved into a hydrogen bond interaction with Thr199 side chain OH. A second hydrogen bond interaction between another boronate oxygen atom and Thr199 backbone amide along with some hydrophobic interactions between the organic scaffold of the inhibitor and residues into the enzyme active site also contributed to the stabilization of the complex (Fig. 4B).

Compounds 1 and 2 differ only in the group at the *para* position relative to the boronic acid moiety (Fig. 2). Thus, the observation that 1 binds the enzyme in its trigonal planar form, whereas 2 binds as a boronate, is quite intriguing, especially because, as seen in the structural superposition reported in Fig. 5, no other significant differences are observed in the position of the organic scaffolds of the two inhibitors in the enzyme active site.

To rule out the possibility that the observed differences were due to varying experimental conditions, particularly the pH values of the crystallization solutions (pH 7.4 in Rasheed's paper and pH 8.5 in our case), we prepared new crystals of the hCA II/2 adduct using the same crystallization solution utilized by Rasheed and colleagues [29]. We collected data up to 1.07 Å resolution and analyzed the structure. Again, our findings showed compound 2 bound to the enzyme active site in its tetrahedral anionic form, with a binding mode perfectly superimposable to that observed at pH 8.5 (Fig. 4C and D).

Thus, in our opinion, considering the significant difference in structural resolution between the previously analyzed hCA II/1 adduct [29] and the hCA II/2 adducts here reported, the observed differences could be ascribed to the lower resolution of the structure of the first adduct which did not allow for an unambiguous interpretation of the electron density. On the contrary, the very high resolution of our structures provides a very clear view of the inhibitor binding mode. It

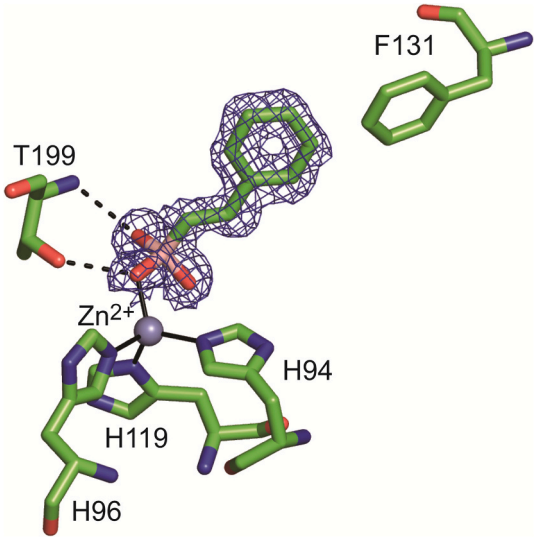


**Fig. 7.** Active site region of the hCA II/3 complex. The σA-weighted (2Fo-Fc) map, contoured at 1.0 σ, relative to the inhibitor, and residues involved in hydrogen bonds and hydrophobic interactions (<4 Å) are shown. Continuous lines indicate zinc ion coordination, whereas dashed lines indicate hydrogen bond distances.

should also be stressed that the findings reported in this paper agree with our previous studies on benzoxaborole derivatives, another class of boronic compounds, known to have good CA inhibition activities [46–48]. Indeed, benzoxaboroles also coordinate the catalytic zinc ion of the CA active site in their tetrahedral anionic form [49–51] (see Fig. 6).

To further characterize boronic acids as CAIs, we also investigated the effect of the nature of the organic scaffold on the binding mode of these molecules to the CA active site. In particular, using the same procedure described for the compound 2, we obtained crystals of the complex between hCA II and an alkenyl-boronic acid, namely *trans*-2-phenylvinylboronic acid (compound 3 in Fig. 2. $K_I$ against hCA II 534 μM) [24]. In this case as well, we obtained very high-resolution data (1.35 Å) and were able to unambiguously determine the binding mode to the active site. As clearly shown in Fig. 7, like compound 2 the phenylvinylboronic acid 3 binds the enzyme in its tetrahedral anionic form and coordinates the zinc ion through one of its hydroxyl oxygens.

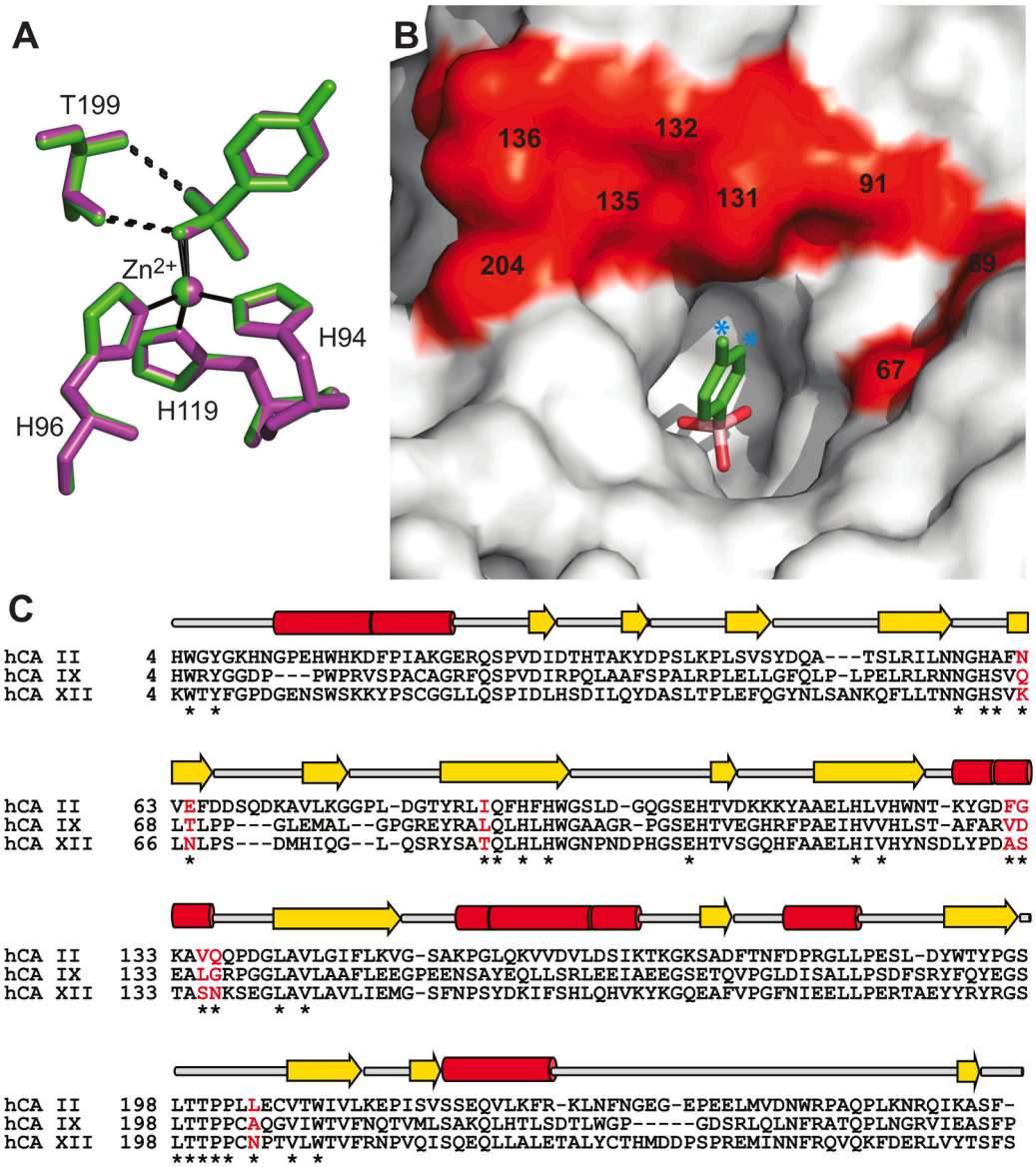


**Fig. 8.** A) Structural superposition of the hCA II/2 adduct (green) with hCA II/4 adduct (PDB code 6GDC, magenta) in the active site region [52]. B) Solvent accessible surface of the protein in the hCA II/2 adduct. Residues of active site which are different between isoforms II, IX, and XII are highlighted in red. Cyan asterisks indicate possible modification sites on the inhibitor phenyl ring for the development of new boronic acid inhibitors. C) Structure-based sequence alignment between hCA II, hCA IX and hCA XII. Residues delimiting the active site cavity are marked with asterisks, those differing between the three isoforms are colored in red, whereas helical regions and beta strands are indicated with red cylinders and yellow arrows, respectively.

These findings further indicate that, regardless of the nature of the organic scaffold, the binding mode of boronic acids to the CA active site is associated with their tetrahedral anionic form. However, based on our observations, it is difficult to establish whether it is the anionic tetrahedral form of these inhibitors that binds directly to the CA active site or if this form is obtained by the reaction of the electron-deficient trigonal planar boron atom with the highly nucleophilic zinc-bound hydroxide anion.

Undoubtedly, in this form boronic acids can optimally interact with the enzyme, establishing, beyond the zinc ion coordination, polar interactions with Thr199 residue, analogous to what is observed in the case of benzenesulfonamides, the CAIs par excellence [13]. This is clearly shown in Fig. 8A which describes the structural superposition of 2 and the simple benzenesulfonamide 4 [52] (Fig. 2), when bound to the hCA II active site. The two inhibitors present an identical binding mode to the enzyme in terms of hydrogen bond network and of orientation of the organic scaffold (Fig. 8A). This observation opens the way for the development of boronic acid derivatives, adopting the same strategy used for benzenesulfonamides, the so-called “tail approach”. This approach involves appending different moieties, referred to as tails, to the phenyl ring to facilitate the interaction of the inhibitor with the more external regions of the hCA active site, which are characterized by the highest variability between the various isoforms [13,53]. In particular, with regard to the tumor-associated hCA IX and hCA XII, the main differences compared to hCA II are placed on the rim of the active site, mainly in the helical region containing residues 131–135 (Fig. 8B and C). The replacement of the methyl group of compound 2 with larger substituents, or the introduction of tails on the phenyl ring in *meta* position relative to the boronic acid moiety, could lead molecules able to interact with this region, thus enhancing their selectivity.

## 4. Conclusion

In conclusion, the data here reported provide evidence that boronic

acids bind to the CA active site in their deprotonated anionic form, forming adducts similar to those formed by classical sulfonamide inhibitors. These data, together with studies previously reported by Winum and colleagues [24,25], strongly indicate the need for further investigations on these molecules aimed at developing new derivatives. By changing or derivatizing the R-group, or introducing tails in the meta position of the phenyl ring, molecules can be developed that are able to interact with the less conserved regions of the active site and finely modulate the affinity toward the different CA isoforms.

## CRediT authorship contribution statement

**Davide Esposito:** Writing – original draft, Investigation. **Simona Maria Monti:** Writing – review & editing, Supervision, Funding acquisition. **Claudiu T. Supuran:** Writing – original draft. **Jean-Yves Winum:** Writing – original draft. **Giuseppina De Simone:** Writing – review & editing, Writing – original draft, Supervision, Funding acquisition, Formal analysis, Data curation. **Vincenzo Alterio:** Writing – review & editing, Writing – original draft, Validation, Supervision, Investigation, Formal analysis, Data curation.

## Declaration of competing interest

The authors declare that they have no known competing financial interests or personal relationships that could have appeared to influence the work reported in this paper.

## Acknowledgements

We would like to acknowledge the Italian National Research Council (CNR) (Joint Bilateral Agreements CNR/CINVESTAV (Mexico) and CNR/PAS (Poland)) for funding this research work.

We also would like to thank Massimiliano Mazzucchi and Giorgio Varriale (Institute of Biostructures and Bioimaging – CNR) for their technical support, Elettra Sincrotrone Trieste for providing access to its synchrotron radiation facilities, and Dr. Nicola Demitri for assistance in using beamline XRD2.

## Data availability

Crystallographic data are available in the RCSB PDB database under the codes: 9GFV, 9GFW, 9GFX.

## References

[1] D.G. Hall, Structure, properties, and preparation of Boronic acid derivatives, Overview of Their Reactions and Applications, in: Boronic Acids Prep. Appl. Org. Synth. Med. (2006), https://doi.org/10.1002/3527606548.ch1.

[2] X. Wang, D. Yue, E. Lv, L. Wu, W. Qin, Reporter-free potentiometric sensing of boronic acids and their reactions by using quaternary ammonium salt-functionalized polymeric liquid membranes, Anal. Chem. 86 (2014) 1927–1931, https://doi.org/10.1021/ac500028v.

[3] M.P. Silva, L. Saraiva, M. Pinto, M.E. Sousa, Boronic acids and their derivatives in medicinal chemistry: synthesis and biological applications, Molecules 25 (2020), https://doi.org/10.3390/molecules25184323.

[4] B.C. Das, M. Adil Shareef, S. Das, N.K. Nandwana, Y. Das, M. Saito, L.M. Weiss, Boron-containing heterocycles as promising pharmacological agents, Bioorg. Med. Chem. 63 (2022) 116748, https://doi.org/10.1016/J.BMC.2022.116748.

[5] S.J. Baker, C.Z. Ding, T. Akama, Y.K. Zhang, V. Hernandez, Y. Xia, Therapeutic potential of boron-containing compounds, future, Med. Chem. 1 (2009) 1275–1288, https://doi.org/10.4155/FMC.09.71.

[6] S. Song, P. Gao, L. Sun, D. Kang, J. Kongsted, V. Poongavanam, P. Zhan, X. Liu, Recent developments in the medicinal chemistry of single boron atom-containing compounds, Acta Pharm. Sin. B 11 (2021) 3035–3059, https://doi.org/10.1016/J.APSB.2021.01.010.

[7] S. Kulkarni, D. Bhandary, Y. Singh, V. Monga, S. Thareja, Boron in cancer therapeutics: an overview, Pharmacol. Ther. 251 (2023) 108548, https://doi.org/10.1016/J.PHARMTHERA.2023.108548.

[8] P.G. Richardson, T. Hideshima, K.C. Anderson, Bortezomib (PS-341): a novel, first-in-class proteasome inhibitor for the treatment of multiple myeloma and other cancers, Cancer Control 10 (2003) 361–369, https://doi.org/10.1177/107327480301000502.

[9] P.G. Richardson, S. Zweegman, E.K. O'Donnell, J.P. Laubach, N. Raje, P. Voorhees, R.H. Ferrari, T. Skacel, S.K. Kumar, S. Lonial, Ixazomib for the treatment of multiple myeloma, Expert. Opin. Pharmacother. 19 (2018) 1949–1968, https://doi.org/10.1080/14656566.2018.1528229.

[10] J. Plescia, N. Moitessier, Design and discovery of boronic acid drugs, Eur. J. Med. Chem. 195 (2020) 112270, https://doi.org/10.1016/J.EJMECH.2020.112270.

[11] A.M. O'Farrell, A. van Vliet, K. Abou Farha, J.M. Cherrington, D.A. Campbell, X. Li, D. Hanway, J. Li, H.P. Guler, Pharmacokinetic and pharmacodynamic assessments of the dipeptidyl peptidase-4 inhibitor PHX1149: double-blind, placebo-controlled, single- and multiple-dose studies in healthy subjects, Clin. Ther. 29 (2007) 1692–1705, https://doi.org/10.1016/J.CLINTHERA.2007.08.005.

[12] D.T. Vogl, T.G. Martin, R. Vij, P. Hari, J.R. Mikhael, D. Siegel, K.L. Wu, M. Delforge, C. Gasparetto, Phase I/II study of the novel proteasome inhibitor delanzomib (CEP-18770) for relapsed and refractory multiple myeloma, Leuk. Lymphoma 58 (2017) 1872–1879, https://doi.org/10.1080/10428194.2016.1263842.

[13] V. Alterio, A. Di Fiore, K. D'Ambrosio, C.T. Supuran, G. De Simone, Multiple binding modes of inhibitors to carbonic anhydrases: how to design specific drugs targeting 15 different isoforms? Chem. Rev. 112 (2012) 4421–4468, https://doi.org/10.1021/cr200176r.

[14] A. Di Fiore, C.T. Supuran, A. Scaloni, G. De Simone, Post-translational modifications in tumor-associated carbonic anhydrases, Amin. Acids 54 (2021) 543–558, https://doi.org/10.1007/S00726-021-03063-Y.

[15] E. Langella, A. Di Fiore, V. Alterio, S.M. Monti, G. De Simone, K. D'Ambrosio, a-CAs from Photosynthetic Organisms, Int. J. Mol. Sci. 23 (2022) 12045, https://doi.org/10.3390/IJMS231912045.

[16] C.T. Supuran, Carbonic anhydrases: novel therapeutic applications for inhibitors and activators, Nat. Rev. Drug Discov. 7 (2008) 168–181, https://doi.org/10.1038/nrd2467.

[17] C.T. Supuran, G. De Simone (Eds.), Carbonic Anhydrases as Biocatalysts, 1st ed., Elsevier, Amsterdam, 2015. https://www.elsevier.com/books/carbonic-anhydrases-as-biocatalysts/supuran/978-0-444-63258-6.

[18] S.C. Chafe, F.S. Vizeacoumar, G. Venkateswaran, O. Nemirovsky, S. Awrey, W. S. Brown, P.C. McDonald, F. Carta, A. Metcalfe, J.M. Karasinska, L. Huang, S. K. Muthuswamy, D.F. Schaeffer, D.J. Renouf, C.T. Supuran, F.J. Vizeacoumar, S. Dedhar, Genome-wide synthetic lethal screen unveils novel CAIX-NFS1/xCT axis as a targetable vulnerability in hypoxic solid tumors, Sci. Adv. 7 (2021) eabj0364, https://doi.org/10.1126/SCIADV.ABJ0364.

[19] P.C. McDonald, S. Chia, P.L. Bedard, Q. Chu, M. Lyle, L. Tang, M. Singh, Z. Zhang, C.T. Supuran, D.J. Renouf, S. Dedhar, A phase 1 study of SLC-0111, a novel inhibitor of carbonic anhydrase IX, in patients with advanced solid tumors, Am. J. Clin. Oncol. Cancer Clin. Trials 43 (2020) 484–490, https://doi.org/10.1097/COC.0000000000000691.

[20] Y. Lou, P.C. McDonald, A. Oloumi, S. Chia, C. Ostlund, A. Ahmadi, A. Kyle, U. Auf Dem Keller, S. Leung, D. Huntsman, B. Clarke, B.W. Sutherland, D. Waterhouse, M. Bally, C. Roskelley, C.M. Overall, A. Minchinton, F. Pacchiano, F. Carta, A. Scozzafava, N. Touisni, J.Y. Winum, C.T. Supuran, S. Dedhar, Targeting tumor hypoxia: suppression of breast tumor growth and metastasis by novel carbonic anhydrase IX inhibitors, Cancer Res. 71 (2011) 3364–3376, https://doi.org/10.1158/0008-5472.CAN-10-4261.

[21] I. Nishimori, A. Innocenti, D. Vullo, A. Scozzafava, C.T. Supuran, Carbonic anhydrase inhibitors. Inhibition studies of the human secretory isoform VI with anions, Bioorg. Med. Chem. Lett. 17 (2007) 1037–1042, https://doi.org/10.1016/J.BMCL.2006.11.028.

[22] A. Innocenti, D. Vullo, J. Pastorek, A. Scozzafava, S. Pastorekova, I. Nishimori, C. T. Supuran, Carbonic anhydrase inhibitors. Inhibition of transmembrane isozymes XII (cancer-associated) and XIV with anions, Bioorg. Med. Chem. Lett. 17 (2007) 1532–1537, https://doi.org/10.1016/J.BMCL.2006.12.113.

[23] A. Innocenti, M. Hilvo, S. Parkkila, A. Scozzafava, C.T. Supuran, Carbonic anhydrase inhibitors: the membrane-associated isoform XV is highly inhibited by inorganic anions, Bioorg. Med. Chem. Lett. 19 (2009) 1155–1158, https://doi.org/10.1016/J.BMCL.2008.12.082.

[24] J.Y. Winum, A. Innocenti, A. Scozzafava, J.L. Montero, C.T. Supuran, Carbonic anhydrase inhibitors. Inhibition of the human cytosolic isoforms I and II and transmembrane, tumor-associated isoforms IX and XII with boronic acids, Bioorg. Med. Chem. 17 (2009) 3649–3652, https://doi.org/10.1016/J.BMC.2009.03.058.

[25] A. Innocenti, J.Y. Winum, R.A. Hall, F.A. Mühlschlegel, A. Scozzafava, C. T. Supuran, Carbonic anhydrase inhibitors. Inhibition of the fungal β-carbonic anhydrases from Candida albicans and Cryptococcus neoformans with boronic acids, Bioorg. Med. Chem. Lett. 19 (2009) 2642–2645, https://doi.org/10.1016/J.BMCL.2009.03.147.

[26] S. Giovannuzzi, A. Nikitjuka, B.R. Pereira Resende, M. Smietana, A. Nocentini, C. T. Supuran, J.Y. Winum, Boron-containing carbonic anhydrases inhibitors, Bioorg. Chem. 143 (2024), https://doi.org/10.1016/J.BIOORG.2023.106976.

[27] C.T. Supuran, Bortezomib inhibits bacterial and fungal β-carbonic anhydrases, Bioorg. Med. Chem. 24 (2016) 4406–4409, https://doi.org/10.1016/J.BMC.2016.07.035.

[28] C.T. Supuran, Bortezomib inhibits mammalian carbonic anhydrases, Bioorg. Med. Chem. 25 (2017) 5064–5067, https://doi.org/10.1016/J.BMC.2016.10.023.

[29] S. Rasheed, N. ul Huda, S.Z. Fisher, S. Falke, S. Gul, M.S. Ahmed, M.I. Choudhary, Identification, crystallization, and first X-ray structure analyses of phenyl boronic acid-based inhibitors of human carbonic anhydrase-II, Int. J. Biol. Macromol. 267 (2024), https://doi.org/10.1016/J.IJBIOMAC.2024.131268.

[30] L. Dzhekieva, M. Rocaboy, F. Kerff, P. Charlier, E. Sauvage, R.F. Pratt, Crystal structure of a complex between the actinomadura R39 dd -peptidase and a peptidoglycan-mimetic boronate inhibitor: interpretation of a transition state

analogue in terms of catalytic mechanism, Biochemistry 49 (2010) 6411–6419, https://doi.org/10.1021/bi100757c.
[31] N.A. Larsen, J.M. Turner, J. Stevens, S.J. Rosser, A. Basran, R.A. Lerner, N.C. Bruce, I.A. Wilson, Crystal structure of a bacterial cocaine esterase, Nat. Struct. Biol. 9 (2001) 17–21, https://doi.org/10.1038/nsb742.
[32] S.W. Yang, J. Pan, Y. Root, G. Scapin, L. Xiao, J. Su, Serendipitous discovery of aryl boronic acids as β-lactamase inhibitors, Bioorg. Med. Chem. Lett. 30 (2020) 126795, https://doi.org/10.1016/J.BMCL.2019.126795.
[33] J.P. Werner, J.M. Mitchell, M.A. Taracila, R.A. Bonomo, R.A. Powers, Exploring the potential of boronic acids as inhibitors of OXA-24/40 β-lactamase, Protein Sci. 26 (2017) 515–526, https://doi.org/10.1002/PRO.3100.
[34] J. Schrader, F. Henneberg, R.A. Mata, K. Tittmann, T.R. Schneider, H. Stark, G. Bourenkov, A. Chari, The inhibition mechanism of human 20S proteasomes enables next-generation inhibitor design, Science (80-. ). 353 (2016) 594–598, https://doi.org/10.1126/science.aaf8993.
[35] W. Minor, M. Cymborowski, Z. Otwinowski, M. Chruszcz, HKL-3000: the integration of data reduction and structure solution – from diffraction images to an initial model in minutes, Acta Crystallogr. D Biol. Crystallogr. 62 (2006) 859–866, https://doi.org/10.1107/S0907444906019949.
[36] A.E. Eriksson, T.A. Jones, A. Liljas, Refined structure of human carbonic anhydrase II at 2.0 a resolution, Proteins 4 (1988) 274–282, https://doi.org/10.1002/PROT.340040406.
[37] G.N. Murshudov, A.A. Vagin, E.J. Dodson, Refinement of macromolecular structures by the maximum-likelihood method, Acta Crystallogr. D Biol. Crystallogr. 53 (1997) 240–255, https://doi.org/10.1107/S0907444996012255.
[38] T.A. Jones, J.-Y. Zou, S.W. Cowan, M. Kjeldgaard, Improved methods for building protein models in electron density maps and the location of errors in these models, Acta Crystallogr. Sect. A 47 (1991) 110–119, https://doi.org/10.1107/S0108767390010224.
[39] R.A. Laskowski, M.W. MacArthur, D.S. Moss, J.M. Thornton, PROCHECK: a program to check the stereochemical quality of protein structures, J. Appl. Crystallogr. 26 (1993) 283–291, https://doi.org/10.1107/S0021889892009944.
[40] R.W.W. Hooft, G. Vriend, C. Sander, E.E. Abola, Errors in protein structures [3], Nature 381 (1996) 272, https://doi.org/10.1038/381272a0.
[41] A. Di Fiore, G. De Simone, V. Alterio, V. Riccio, J.Y. Winum, F. Carta, C.T. Supuran, The anticonvulsant sulfamide JNJ-26990990 and its S,S-dioxide analog strongly inhibit carbonic anhydrases: solution and X-ray crystallographic studies, Org. Biomol. Chem. 14 (2016) 4853–4858, https://doi.org/10.1039/C6OB00803H.
[42] V. Alterio, M. Tanc, J. Ivanova, R. Zalubovskis, I. Vozny, S.M. Monti, A. Di Fiore, G. De Simone, C.T. Supuran, X-ray crystallographic and kinetic investigations of 6-sulfamoyl-saccharin as a carbonic anhydrase inhibitor, Org. Biomol. Chem. 13 (2015) 4064–4069, https://doi.org/10.1039/C4OB02648A.
[43] V. Alterio, D. Esposito, S.M. Monti, C.T. Supuran, G. De Simone, Crystal structure of the human carbonic anhydrase II adduct with 1-(4-sulfamoylphenyl-ethyl)-2,4,6-triphenylpyridinium perchlorate, a membrane-impermeant, isoform selective inhibitor, J. Enzyme Inhib. Med. Chem. 33 (2018) 151–157, https://doi.org/10.1080/14756366.2017.1405263.
[44] A. Angeli, L. Micheli, R. Turnaturi, L. Pasquinucci, C. Parenti, V. Alterio, A. Di Fiore, G. De Simone, S.M. Monti, F. Carta, L. Di Cesare Mannelli, C. Ghelardini, C. T. Supuran, Discovery of a novel series of potent carbonic anhydrase inhibitors with selective affinity for μ opioid receptor for safer and long-lasting analgesia, Eur. J. Med. Chem. 260 (2023) 115783, https://doi.org/10.1016/J.EJMECH.2023.115783.
[45] E. Langella, D. Esposito, S.M. Monti, C.T. Supuran, G. De Simone, V. Alterio, A combined in silico and structural study opens new perspectives on aliphatic sulfonamides, a still poorly investigated class of CA inhibitors, Biol 12 (2023) 281, https://doi.org/10.3390/BIOLOGY12020281.
[46] A. Bonardi, A. Nocentini, R. Cadoni, S. Del Prete, P. Dumy, C. Capasso, P. Gratteri, C.T. Supuran, J.Y. Winum, Benzoxaboroles: new potent inhibitors of the carbonic anhydrases of the pathogenic bacterium vibrio cholerae, ACS Med. Chem. Lett. 11 (2020) 2277–2284, https://doi.org/10.1021/ACSMEDCHEMLETT.0C00403.
[47] A. Nocentini, R. Cadoni, S. Del Prete, C. Capasso, P. Dumy, P. Gratteri, C. T. Supuran, J.Y. Winum, Benzoxaboroles as efficient inhibitors of the β-carbonic anhydrases from pathogenic Fungi: activity and modeling study, ACS Med. Chem. Lett. 8 (2017) 1194–1198, https://doi.org/10.1021/ACSMEDCHEMLETT.7B00369.
[48] A. Larcher, A. Nocentini, C.T. Supuran, J.Y. Winum, A. Van Der Lee, J.J. Vasseur, D. Laurencin, M. Smietana, Bis-benzoxaboroles: design, synthesis, and biological evaluation as carbonic anhydrase inhibitors, ACS Med. Chem. Lett. 10 (2019) 1205–1210, https://doi.org/10.1021/ACSMEDCHEMLETT.9B00252.
[49] E. Langella, V. Alterio, K. D'Ambrosio, R. Cadoni, J.Y. Winum, C.T. Supuran, S. M. Monti, G. De Simone, A. Di Fiore, Exploring benzoxaborole derivatives as carbonic anhydrase inhibitors: a structural and computational analysis reveals their conformational variability as a tool to increase enzyme selectivity, J. Enzyme Inhib. Med. Chem. 34 (2019) 1498, https://doi.org/10.1080/14756366.2019.1653291.
[50] A. Nocentini, A. Bonardi, C. Bazzicalupi, V. Alterio, D. Esposito, S.M. Monti, M. Smietana, G. De Simone, C.T. Supuran, P. Gratteri, J.Y. Winum, 6-Substituted Triazolyl Benzoxaboroles as Selective Carbonic Anhydrase Inhibitors: In Silico Design, Synthesis, and X-ray Crystallography, J. Med. Chem. 66 (2023) 8118–8129, https://doi.org/10.1021/ACS.JMEDCHEM.3C00433.
[51] V. Alterio, R. Cadoni, D. Esposito, D. Vullo, A. Di Fiore, S.M. Monti, A. Caporale, M. Ruvo, M. Sechi, P. Dumy, C.T. Supuran, G. De Simone, J.Y. Winum, Benzoxaborole as a new chemotype for carbonic anhydrase inhibition, Chem. Commun. (Camb.) 52 (2016) 11983–11986, https://doi.org/10.1039/C6CC06399C.
[52] S. Glöckner, K. Ngo, C.P. Sager, T. Hüfner-Wulsdorf, A. Heine, G. Klebe, Conformational changes in alkyl chains determine the thermodynamic and kinetic binding profiles of carbonic anhydrase inhibitors, ACS Chem. Biol. 15 (2020) 675–685, https://doi.org/10.1021/acschembio.9b00895.
[53] A. Scozzafava, L. Menabuoni, F. Mincione, F. Briganti, G. Mincione, C.T. Supuran, Carbonic anhydrase inhibitors. Synthesis of water-soluble, topically effective, intraocular pressure-lowering aromatic/heterocyclic sulfonamides containing cationic or anionic moieties: is the tail more important than the ring? J. Med. Chem. 42 (1999) 2641–2650, https://doi.org/10.1021/JM9900523.